Superconducting properties of barium in three phases under high pressure from first principles*

Zhou Da-Wei(周大伟)[a)†], Pu Chun-Ying(濮春英)[a)], Song Hai-Zhen(宋海珍)[a)], Li Gen-Quan(李根全)[a)], Song Jin-Fan(宋金璠)[a)], Lu Cheng(卢 成)[a)], and Bao Gang(包 刚)[b)]

[a)] College of Physics and Electronic Engineering, Nanyang Normal University, Nanyang 473061, China
[b)] College of Physics and Electronic Information, Inner Mongolia University for the Nationalities, Tongliao 028043, China

(Received 30 November 2012; revised manuscript received 1 January 2013)

Electron–phonon coupling (EPC) in the three high-pressure phases of Ba is investigated using a pseudopotential plane-wave method based on density functional perturbation theory. The calculated values of superconducting critical temperature T_c of Ba–I and Ba–II under pressure are consistent well with the trends observed experimentally. Moreover, Ba–V is found to be superconducting with a maximum T_c exceeding 7.8 K at 45 GPa. With the increase of pressure, the values of T_c increase in Ba I and Ba–II but the value of T_c decreases in Ba–V. For Ba–I at pressures below 2 GPa, the increases of logarithmic average frequency $\omega_{\log}$ and electron–phonon coupling parameters λ both contribute to the enhancement of T_c. For all the three phases at pressures above 2 GPa, T_c is found to be primarily determined by λ. Further investigation reveals that for all the three phases, the change in λ with pressure can be explained mainly by change in the phonon frequency. Thus for Ba–II and Ba–V, although they exhibit completely different superconducting behaviors, their superconductivities have the same origin; the pressure dependence of T_c is determined finally by the pressure dependence of phonon frequency.

Keywords: high-pressure phase transition, superconductivity, lattice dynamics

PACS: 74.25.Dw, 74.62.Fj, 71.15.Mb **DOI:** 10.1088/1674-1056/22/8/087403

1. Introduction

Superconductivity in an elemental solid at high pressure is a subject of great importance and is believed to be related to the general area of electron–phonon coupling (EPC) in solids. Among those superconducting elements, the alkaline-earth metals such as Ca,[1,2] Sr, and Ba[3] occupy a special position. They are not superconducting at ambient pressure but become superconductors under appropriate pressures. The pressure-induced superconductivities were believed to be caused by the pressure-driven electronic s→d transfer.[4–6] With pressure increasing, the amount of d electronic occupation of those elements increases, which changes the bonding characteristics and finally causes the structural phase transition and superconductivity. Both Ca and Sr crystallize into face-centred cubic (fcc) structures at ambient pressure and transform into body-centred cubic (bcc) structures at higher pressure.[6] The fcc–bcc transition in Ca and Sr was explained by the increase of d electronic occupation number under pressures.[4] Ba behaves slightly differently, the amount of d occupation of electrons in Ba is higher than that in Ca and Sr, thus Ba already adopts bcc (Ba–I) lattice at ambient pressure, and transforms into Ba–II at 5.5 GPa with a hexagonal close packed lattice (hcp).[7] Further compression to 12.5 GPa leads to the observation of a third phase transition to Ba–IV, a complex incommensurate tetragonal host–guest lattice.[8,9] Ba–V exists above 45 GPa, which also adopts the hcp structure, and the stability range of Ba–V phase is found to extend to the megabar regime.[10]

The increase of the d-band occupation number of electrons under pressure may also increase the value of T_c.[6] Ca was first observed to be superconducting at 2 K at 44 GPa.[1] The T_c increases almost linearly with pressure up to 15 K at about 150 GPa.[2] and reaches about 25 K under further compression to 161 GPa.[11] Up to now, it is the highest T_c found in elemental solids. Compared with Ca, Ba becomes superconducting at relatively low pressures below 2 GPa.[12] The value of T_c increases with pressure increasing, and reaches a maximum in Ba–IV, where the s–d electron transfer is considered to be completed.[8,9] After that, Ba–V adopts hcp structure, so does Ba–II.[10] No further experiments suggest whether Ba–V is still superconducting. Moreover, although numerous experimental and theoretical investigations have been carried out on the structural or electronic properties of Ba;[3,7,8,10,13–17] besides, the superconductivity was believed to be related to s–d electron transfer, as far as we know, there has been no more theoretical study of the superconductivity in Ba under pressure. In fact, for the phonon-mediated superconducting

*Project supported by the National Natural Science Foundation of China (Grant Nos. 11247222, 11164020, and 51001042), the Nanyang Normal University Science Foundation, China (Grant Nos. ZX2012018, ZX2010011, and nytc2006k102), the Natural Science Foundation of Science and Technology Department of Henan Province, China (Grant Nos. 112102210019 and 112300410121), the Natural Science Foundation of Education Department of Henan Province, China (Grant Nos. 2011B140015 and 2010B140012), the Higher Education Reform of Henan Province, China (Grant Nos. 2012SJGLX233), the China Postdoctoral Science Foundation (Grant No. 20110491317), and the Young Core Instructor Foundation from the Education Department of Henan Province, China (Grant No. 2012GGJS-152).

†Corresponding author. E-mail: zhoudawei@nynu.edu.cn

© 2013 Chinese Physical Society and IOP Publishing Ltd

superconductor, Bardeen–Cooper–Schrieffer (BCS) theory[18] can provide a successful description, thus we can investigate the origin of superconductivity in Ba based on the BCS theory. Understanding the origin of the superconductivity in Ba under high pressure is the main motivation for the study presented here, and besides the superconducting properties, the relation between electron–phonon coupling and lattice dynamics in barium is also investigated in detail to better understand the superconducting behavior.

2. Computational method

Lattice parameters, enthalpy curve, phonon curves, and electron–phonon coupling interaction are calculated using the QUANTUM ESPRESSO package.[19] In these calculations, the generalized gradient approximation (GGA)[20] exchange–correlation functional in the Troullier–Martins form[21] is employed. Convergence tests give a kinetic energy cutoff as 50 Ry. For Ba–I, a $14\times14\times14$ Monkhorst–Pack (MP)[22] grid for the electronic Brillouin zone (BZ) integration, and a $7\times7\times7$ Q mesh are used for both phonon and EPC calculations. At each Q point, the phonon and EPC matrices are calculated with $21\times21\times21$ Q-point meshes, while for Ba–II and Ba–V, a $14\times14\times8$ MP grid for the electronic BZ integration, and a $7\times7\times4$ Q mesh are used for both phonon and EPC calculations. At each Q point, the phonon and EPC matrices are calculated with $21\times21\times12$ Q-point meshes, accordingly. The convergences of the plane-wave basis set and MP sampling are examined by employing a higher kinetic energy cutoff and a denser grid set.

3. Results and discussion

The calculated enthalpy of Ba–II relative to that of Ba–I is shown in the inset of Fig. 1. Ba–I transforms into Ba–II at about 3.9 GPa. The calculated transition pressure is smaller than the experimental value of 5.5 GPa.[4] However, our results are closer to the experimental value than the previous theoretical value (2.8 GPa).[13] An interesting phenomenon in barium under high pressure is that although both Ba–II and Ba–V adopt the same hcp structure, they exhibit different bonding properties and high-pressure behaviors. The pressure dependence of c/a ratio in Ba–II decreases dramatically from 1.58 to 1.50, whereas the c/a ratio in Ba–V is almost pressure-independent at about 1.58.[10] To verify the rationality of our calculations, we calculate the c/a ratio of the two hcp-Ba as a function of pressure. The results together with the experimental values [10] and other theoretical results[9,13,17] are listed in Fig. 1. The theoretical results calculated by Reed and Ackland[9] using the ultra-soft pseudopotentials,[23] have relatively large errors in both Ba–II and Ba–V. While the two other results calculated by Jona and Marcus[13] and Zeng *et al.*[17] using the more accurate full-potential methods were closer to the experimental measures. In this paper, we calculate the c/a ratio by means of the accurate Troullier–Martins norm-conserving pseudopotential.[21] The calculated results below 15 GPa accord well with experimental measures. Above 45 GPa, the calculated c/a ratio is almost pressure-independent with a value of about 1.6, which is also in good agreement with the experimental value of 1.58. All the above results indicate that our calculations can reproduce correctly the high-pressure behavior of Ba.

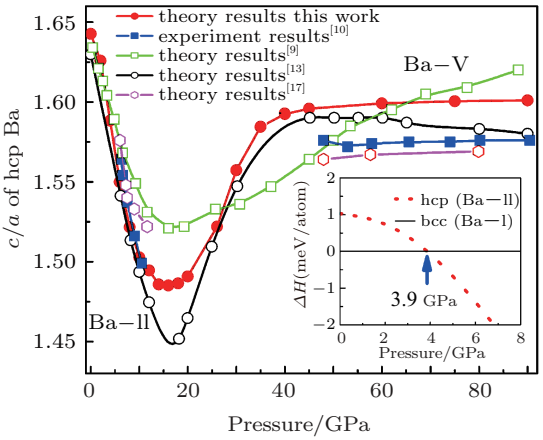


Fig. 1. (color online) Pressure dependences of axial ratio c/a of hcp Ba. Inset shows the enthalpy of Ba–II relative to Ba–I as a function of pressure.

We estimate the T_c in the three phases of Ba using the Allen–Dynes modified McMillan equation,

$$T_c = \frac{\omega_{\log}}{1.2}\exp\left[-\frac{1.04(1+\lambda)}{\lambda-\mu^*(1+0.62\lambda)}\right], \tag{1}$$

where λ is the electron–phonon coupling constant, $\omega_{\log}$ the logarithmic average of the phonon frequency, and μ^* the effective Coulomb pseudopotential. The latter one is defined as $1/\mu^* = 1/\mu + \ln(\omega_{el}/\omega_{ph})$, where μ is the direct Coulomb repulsion between paired electrons, ω_{el} corresponds to a plasma frequency, while ω_{ph} is the high-frequency cutoff in EPC spectral function $\alpha^2F(\omega)$.[24] Moreover, according to the well-known McMillan formula,[25,26] λ can be further expressed as

$$\lambda = \frac{N(E_F)\langle I^2\rangle}{M\langle\omega^2\rangle}, \tag{2}$$

where $N(E_F)$ is the electronic density of states per spin at the Fermi level, $\langle I_i^2\rangle$ the square of the EPC matrix element at $N(E_F)$, M the mass of the atoms, and $\langle\omega^2\rangle$ the average of the squared phonon frequencies. The calculated values of T_c together with the previous theoretical and experimental data are shown in Fig. 2. The pressurized Ba becomes superconducting at relatively low pressures below 2 GPa. Although the T_c in Ba–I continues to increase as pressure increases, as a whole, Ba–I has a very low T_c (below 0.6 K). After Ba–I transforms into Ba–II under further compression, the T_c also continues to increase with pressure increasing, which is in good agreement

with the experimental results.[3] Above 45 GPa, Ba–V is found to be superconducting. The T_c decreases as pressure increases, leading to the final suppression of the superconductivity above 250 GPa. To estimate T_c, the effective Coulomb repulsion parameter μ^* must be appropriately chosen. According to the previous results for a similar system such as Ca[27] and the experimental results in Ref. [3], it is reasonable to choose μ^* to be 0.10 or 0.12. By using a nominal Coulomb repulsion parameter μ^* of 0.10, the maximal T_c in Ba–V is predicted to be 9.5 K at 45 GPa. However, if we assume 0.14 for the value of μ^*, we will obtain a much smaller T_c value of 7.8 K.

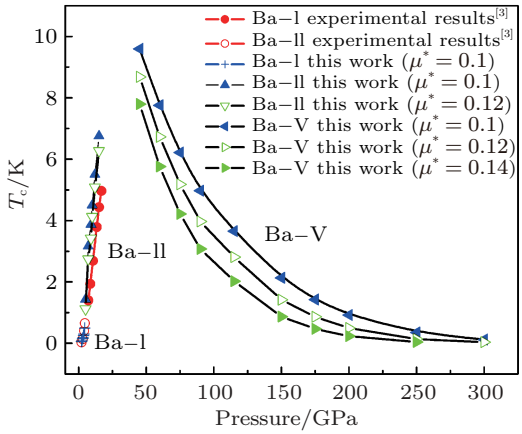


Fig. 2. (color online) Superconducting temperatures versus pressure for the three high-pressure phases in Ba, showing the experimental data and results calculated based on Allen–Dynes equation for different values of $\mu*$.

For many materials, applying pressure can cause great change in T_c.[28–39] Ba is just a typical example, which exhibits complex superconducting behavior under pressure. As pressure increases, the T_c in Ba first increases, then decreases, and finally disappears. Moreover, even having the same hcp structure, Ba–II and Ba–V show completely different superconducting behaviors under pressure. With the increase of pressure, the T_c increases in Ba–II while decreases in Ba–V. To uncover the nature of the complex superconducting behavior, we calculate EPC parameter λ, N_{EF}, and ω_{log} each as a function of pressure, which are shown in Fig. 3. For all the three phases, N_{EF} continues to decrease as pressure increases, according to Eq. (2), the N_{EF} decreases in the direction of lowering T_c. For Ba–I at pressures below 2 GPa, ω_{log} and λ increase with pressure increasing, both of them contribute to the enhancement of T_c. However, ω_{log} changes more gently at pressures above 2 GPa, and even decreases above 3 GPa. Therefore, for Ba–I above 2 GPa, the increasing T_c is not caused by ω_{log}, λ is responsible for the enhancement of T_c. After Ba–I transforms into Ba–II at 3.9 GPa, ω_{log} almost decreases linearly with pressure, thus the dominant cause of the enhancement of T_c is the large increase of λ. For Ba–V, the T_c continues to decrease as pressure increases. From Fig. 3, we can see that with the increase of pressure, ω_{log} increases while λ decreases, thus λ mainly dominates the superconducting behavior of Ba–V, leading to the decrease or even disappearance of T_c.

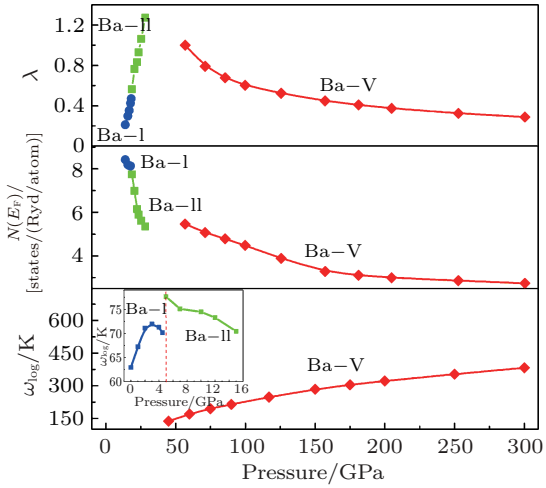


Fig. 3. (color online) The calculated EPC parameter λ, electronic density of states at Fermi level $N(E_F)$, and phonon frequency logarithmic average ω_{log} each as a function of pressure for the three high-pressure phases of Ba.

To further understand the electron–phonon coupling mechanism in detail, we calculate the phonon curves and λ parameters for the three high-pressure phases along several high symmetry lines, which are presented in Figs. 4(a)–4(c) respectively. Although all the three phases are dynamically stable at 0 K, phonon softening can be observed in both Ba–I and Ba–II. The dynamic and mechanical stabilities of the three high-pressure phases in Ba under pressure have been discussed in our previous work.[40] The regions where the phonon softening occurs are circled in black in the corresponding phonon band structures (see Figs. 4(a) and 4(b) in detail). According to Eq. (2), phonon softening (decrease of $\langle\omega^2\rangle$) contributes to the increase of λ, thus for both Ba–I and Ba–II, phonon softening is responsible for the enhancement of λ, leading to the increase of T_c from 2 GPa to 15 GPa. On the contrary, for Ba–V, the pressure-induced phonon hardening results in the decrease of λ, leading to the decrease or even disappearance of T_c. Thus for Ba–II and Ba–V, although they exhibit completely different superconducting behaviors under pressure, their superconductivities have the same origin, the pressure dependence on T_c is determined by the pressure dependence of λ and hence the pressure dependence of phonon frequency.

We also perform the calculations of the spectral function $\alpha^2F(\omega)$ and the integrated EPC parameter λ each as a function of frequency for all the three phases, which are presented in Figs. 5(a)–5(c) respectively. For Ba–I at 3 GPa, a narrow band between 1 THz and 1.5 THz and centers at 1.2 THz contributes most to the EPC. The integrated λ over this fre-

quency range is 0.21, which constitutes 57% of the total coupling parameter. Interestingly, the narrow band is just located in the frequency range where phonon softening occurs in Ba–I, moreover, as pressure increases, the narrow band increases more rapidly, indicating that the phonon softening contributes most to the increase in EPC. A similar phenomenon can be found in Ba–II as shown in Fig. 5(b), the narrow band between 0.6 THz and 1.5 THz contributes most to the EPC. While for Ba–V, all the values of integrated EPC parameter λ at different pressures almost lineally increase with frequency increasing (see Fig. 5(c) in detail). All of the phonon modes nearly have the same contributions to λ.

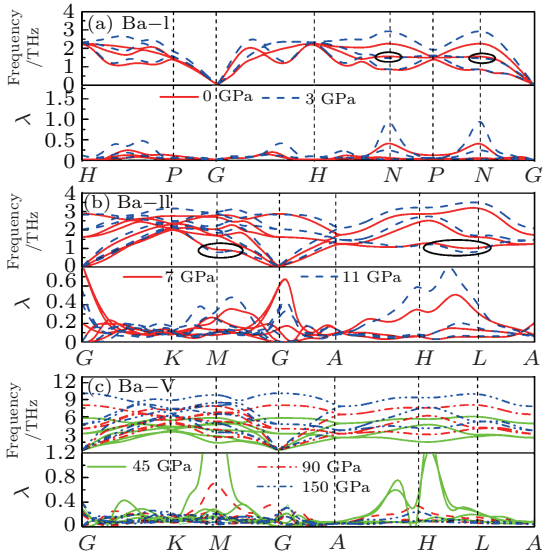


Fig. 4. (color online) Calculated partial EPC constants and phonon spectra of the three high-pressure phases of Ba along the same high symmetry lines at selected pressures in panels (a), (b), and (c), respectively.

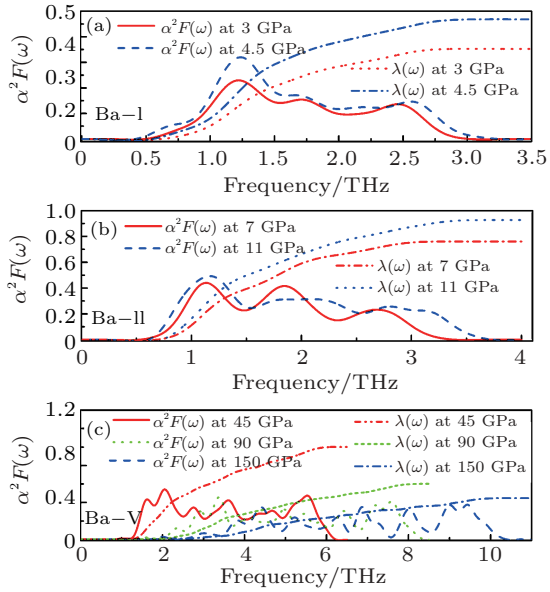


Fig. 5. (color online) Calculated values of Eliashberg phonon spectral function $\alpha^2F(\omega)$ and the electron–phonon integral λ at different pressures for the three high-pressure phases of Ba at selected pressures in panels (a), (b), and (c), respectively.

4. Conclusions

In this paper, we present an extensive study on the electron–phonon coupling of three high-pressure phases of Ba using density functional perturbation theory. We successfully reproduce the superconducting behaviors observed in Ba–I and Ba–II under pressure, and predict the superconducting behavior of Ba–V. The predicted maximal T_c in Ba–V exceeds 7.8 K at 45 GPa. For Ba–I at pressures below 2 GPa, the increases in both $\omega_{\log}$ and λ are responsible for the enhancement of T_c. However, as pressure increases above 2 GPa, λ dominates the superconducting behaviors of the three phases. Moreover, the changes in λ can be explained by the changes in phonon frequency for all the three phases. With pressure increasing, the phonon softening is found in both Ba–I and Ba–II, leading to the increase of λ; while the phonon hardening is found in Ba–V, leading to the decrease of λ. So for Ba–II and Ba–V, although they exhibit completely different superconducting behaviors under pressure, their superconductivities have the same origin, the pressure dependence of T_c is determined by the pressure dependence of λ and hence the pressure dependence of the phonon frequency. Further experiments are suggested to test theoretical results on the electron–phonon interaction and superconducting properties.

References

[1] Dunn K J and Bundy F P 1981 *Phys. Rev. B* **24** 1643
[2] Okada S, Shimizu K, Kobayashi T C, Amaya K and Endo S 1996 *J. Phys. Soc. Jpn.* **65** 1924
[3] Dunn K J and Bundy F P 1982 *Phys. Rev. B* **25** 194
[4] Maksimov E G, Magnitskaya M V and Fortov V E 2007 *Phys. Usp.* **48** 761
[5] Skriver H L 1982 *Phys. Rev. Lett.* **49** 1768
[6] Olijnyk H and Holzapfel W B 1984 *Phys. Lett. A* **100** 191
[7] Barnett J D, Bennion R B and Hall H T 1963 *Science* **141** 534
[8] Nelmes R, Allan D, McMahon M and Belmonte S 1999 *Phys. Rev. Lett.* **83** 4081
[9] Reed S K and Ackland G J 2000 *Phys. Rev. Lett.* **84** 5580
[10] Kenichi T 1994 *Phys. Rev. B* **50** 16238
[11] Yabuuchi T, Matsuoka T, Nakamoto Y and Shimizu K 2006 *J. Phys. Soc. Jpn.* **75** 083703
[12] Moodenbaugh A R and Wittig J 1973 *J. Low. Temp. Phys.* **10** 203
[13] Jona F and Marcus P M 2006 *Europhys. Lett.* **74** 83
[14] Olijnyk H, Nakano S and Takemura K 2007 *Solid State Commun.* **142** 41
[15] Loa I, Nelmes R J, Lundegaard L F and McMahon M 2012 *Nat. Mater.* **11** 627
[16] Jona F and Marcus P M 2006 *J. Phys.: Condens. Matter* **18** 4623
[17] Zeng W S, Heine V and Jepsen O 1999 *J. Phys.: Condens. Matter* **9** 3489
[18] Bardeen J, Cooper L N and Schrieffer J R 1957 *Phys. Rev.* **108** 1175
[19] Giannozzi P, Baroni S, Bonini N, Calandra M, Car R, Cavazzoni C, Ceresoli D, Chiarotti G L, Cococcioni M, Dabo I, Dal Corso A, de Gironcoli S, Fabris S, Fratesi G, Gebauer R, Gerstmann U, Gougoussis C, Kokalj A, Lazzeri M, Martin-Samos L, Marzari N, Mauri F, Mazzarello R, Paolini S, Pasquarello A, Paulatto L, Sbraccia C, Scandolo S, Sclauzero G, Seitsonen A P, Smogunov A, Umari P and Wentzcovitch R M 2009 *J. Phys.: Condens. Matter* **21** 395502
[20] Perdew J P, Burke K and Ernzerhof M 1996 *Phys. Rev. Lett.* **77** 3865
[21] Troullier N and Martins J L 1991 *Phys. Rev. B* **43** 1993
[22] Monkhorst H J and Pack J D 1976 *Phys. Rev. B* **13** 5188
[23] Vanderbilt D 1990 *Phys. Rev. B* **41** 7892
[24] Allen P B and Dynes R C 1975 *Phys. Rev. B* **12** 905

[25] McMillan W L 1968 *Phys. Rev.* **167** 331
[26] Suzuki N and Otani M 2007 *J. Phys.: Condens. Matter* **19** 125206
[27] Yao Y S, Tse J S, Song Z, Klug D D, Sun J and Le Page Y 2008 *Phys. Rev. B* **78** 054506
[28] Buzea C and Robbie K 2005 *Supercond. Sci. Technol.* **18** R1
[29] Tian F B, Wang J H, He Z, Ma Y M, Wang L C, Cui T, Chen C B, Liu B B and Zou G T 2008 *Phys. Rev. B* **78** 235431
[30] Jin X L, Meng X, He Z, Ma Y M, Liu B B, Cui T, Zou G T and Mao H K 2010 *Proc. Natl. Acad. Sci. USA* **107** 9969
[31] Gao G Y, Oganov A R, Bergara A, Martinez-Canales M, Cui T, Iitaka T, Ma Y M and Zou G T 2008 *Phys. Rev. Lett.* **101** 107002
[32] Li Y W, Gao G Y, Xie Y, Ma Y M, Cui T and Zou G T 2010 *Proc. Natl. Acad. Sci. USA* **107** 15708
[33] Xu Y, Tse J S, Oganov A R, Cui T, Wang H, Ma Y and Zou G 2009 *Phys. Rev. B* **79** 144110
[34] Gao G Y, Wang H, Bergara A, Li Y W, Liu G T and Ma Y M 2011 *Phys. Rev. B* **84** 064118
[35] Chan K T, Malone B D and Cohen M L 2012 *Phys. Rev. B* **86** 094515
[36] Wang Y C, Lü J, Ma Y M, Cui T and Zou G T 2009 *Phys. Rev. B* **80** 092505
[37] Xie Y, Oganov A R and Ma Y M 2010 *Phys. Rev. Lett.* **104** 177005
[38] Zhang L J, Xie Y, Cui T, Li Y, He Z, Ma Y M and Zou G T 2006 *Phys. Rev. B* **74** 184519
[39] Duan D F, Jin X, Ma Y M, Cui T, Liu B B and Zou G T 2009 *Phys. Rev. B* **79** 064518
[40] Zhou D W, Lu C, Li G Q, Song J F, Song Y L and Bao G 2012 *Acta Phys. Sin.* **61** 146301 (in Chinese)